



EXPERIMENTAL STUDY OF COMPRESSIVE FAILURE OF CONCRETE UNDER STATIC AND DYNAMIC LOADS

L. Liu¹, H.M. An^{2*}

Abstract: The fracture and fragmentation of concrete under static and dynamic loads are studied. The uniaxial compressive strength test is employed to study the concrete behavior under static loads while the split Hopkinson pressure bar is used to study the dynamic behavior of the concrete under static loads. The theories for acquiring the stress, strain and strain rate of the concrete in the dynamic test by Hopkinson pressure bar has been introduced. The fracture patterns of the concrete in the uniaxial compressive test have been obtained and the static concrete compressive strengths have been calculated. The fracture patterns of the concrete in the uniaxial compressive test have been obtained and the static concrete compressive strengths have been calculated. The fracture and fragmentation of the specimen under dynamic loads have been acquired and the stress-strain curves of concrete under various impact loads are obtained. The stress-strain curve indicates a typical brittle material failure process which includes existing micro-fracture closure stage, linear-elastic stage, nonlinear-elastic stage, and post-failure stages. The influence of the loading rate for the compressive strength of the concrete has compared. Compared with the concrete under static loads, the dynamic loads can produce more fractures and fragments. The concrete strength is influenced by the strain rate and the strength increases almost linearly with the increase of the strain rate.

Keywords: Concrete, Uniaxial compressive strength, Dynamic load, Strain rate, Fracture and fragmentation

¹ A/Prof., PhD., Eng., Kunming University of Science and Technology, Faculty of Land Resource Engineering, 650093, Kunming, China.

² Lecturer, PhD., Eng., Kunming University of Science and Technology, Faculty of Public Security and Emergency Management, 650093, Kunming, China. H.M. An (Huaming An) is the corresponding author.

* Corresponding author (H.M.An): Email Huaming.an@yahoo.com

1. INTRODUCTION

Geo-structures are increasingly needed as modern society develops rapidly [1]. Meanwhile, accidents caused by the fracture and collapse of geo-structures occur frequently. As concrete is one of the most common materials, it is widely used in modern infrastructure. In order to avoid accidents happening, it is important to predict the fracture, failure and collapse behaviour of concrete under different loading rates. In addition, understanding the fracture mechanism of concrete is essential in terms of risk prevention of infrastructure. As a majority of accidents related to the fracture or collapse of the infrastructure is caused by dynamic loads, many researchers have deeply studied the mechanism of the fracture of rock due to dynamic loads. Zhao (2000) conducted the uniaxial and triaxial compressive strength test of the Bukit Timah granite of Singapore. The results show that the compressive strength will increase due to the increased loading rate [2]. The effects of the loading rates of the rock are also studied by Zhang (2000) and it is showed that the cracks of the rock increase with increasing loading rate [3]. Other researches also concluded that the loading rate significantly influences the behavior of the brittle materials [2-10]. However, the current research is still far from enough for a good understanding of the mechanism of rock fracture, failure, and collapse under different loading rates. Thus this paper focuses on the study of concrete behaviors under static and dynamic loads.

2. METHODOLOGY

In this section, the methodologies for rock mechanism test under static and dynamic loads are introduced. The uniaxial compressive strength test is employed to model the rock fracture process under static load while the split Hopkinson pressure bar is used to carry out the dynamic rock fracture test.

2.1. UNIAXIAL COMPRESSIVE STRENGTH TEST UNDER STATIC LOADS

Figure 1 illustrates the geometrical model for the uniaxial compressive strength test under static load. The specimen strength can be calculated by Eq. 2.1 as follows.

$$(2.1) \quad \sigma_c = \frac{P}{A}$$

where P is the force from the top and bottom of the sample and A is the cross section area of top and bottom parts of the specimen.

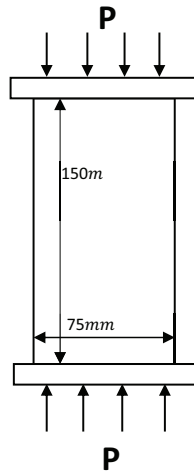


Figure 1. Geometrical model for the uniaxial compressive strength test

2.2. UNIAXIAL COMPRESSIVE STRENGTH TEST UNDER DYNAMIC LOADS

Figure 2 illustrates the schematic of the conventional split Hopkinson pressure bar (SHPB). The main component of SHPB are striker bar, incident bar and transmission bar. The specimen is placed between the incident bar and transmission bar. Figure 3 demonstrates the stress propagation and reflection in the incident bar, specimen and transition bar. A compressive stress pulse wave of approximately one-dimensional propagation is generated in the incident bar when the striker bar hits the incident bar. As can be seen in Figure 3 that the incident bar and the transition bar are in contact (the 1-1 interface in Figure 3). When the stress propagates to the interface, a part of the compressive stress pulse wave continues to propagate into the sample, and the other part is reflected back into the incident bar since the material of the sample is different from the incident bar in terms of wave impedance.

When the compressive stress pulse wave propagating into the rock sample reaches the contact surface of the sample and the transmission bar (the 2-2 interface in Figure 3), reflection and transmission are generated. A portion of the compressive stress pulse wave is reflected back into the sample at interface 2-2 while the other portion is transmitted into the transmission bar. When the compressive stress pulse

wave is reflected back and forth for 3 to 6 times through the interfaces 1-1 and 2-2 in the rock sample, the stress equilibration is established in the rock sample.

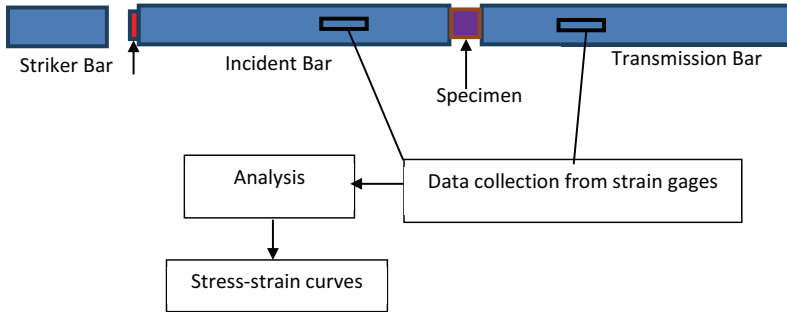


Figure 2. Schematic of conventional split Hopkinson pressure bar (SHPB)

In Figure 3 the cross-sectional area of the incident bar and the transmission bar is A_0 . The cross-sectional area and length of the specimen are A and L . The stress at the interface of 1-1 is $\sigma_1(t)$, while the stress at the interface of 2-2 is $\sigma_2(t)$, and the stress of the specimen is $\sigma(t)$. The wave velocity and the elastic modulus of the incident bar and the transmission bar are C_0 and E_0 respectively, and the strain of the incident wave in the incident bar is ε_i and the reflected wave strain is ε_r . The transmission wave in the transmission rod is ε_t . The mass velocity at the interface of specimen 1-1 is u_1 , and the particle velocity at the interface of specimen 2-2 is u_2 . If the average strain in the specimen is ε , the strain rate is $\dot{\varepsilon}$. Based on the continuity condition of displacement and the one-dimensional stress hypothesis of stress wave, the following equations can be achieved.

Velocity on the interface 1-1:

$$(2.2) \quad u_1(t) = C_0 [\varepsilon_i(t) - \varepsilon_r(t)]$$

Velocity on the interface 2-2:

$$(2.3) \quad u_2(t) = C_0 \varepsilon_t(t)$$

Strain rate in the rock sample:

$$(2.4) \quad \dot{\varepsilon}(t) = \frac{u_1(t) - u_2(t)}{L} = \frac{C_0}{L} [\varepsilon_i(t) - \varepsilon_r(t) - \varepsilon_t(t)]$$

Strain during time t :

$$(2.5) \quad \varepsilon(t) = \frac{C_0}{L} \int_0^t [\varepsilon_i(t) - \varepsilon_r(t) - \varepsilon_t(t)] dt$$

Stress on 1-1 interface :

$$(2.6) \quad A\sigma_1(t) = A_0 E_0 [\varepsilon_i(t) + \varepsilon_r(t)]$$

Stress on 1-1 interface :

$$(2.7) \quad A\sigma_2(t) = A_0 E_0 \varepsilon_t$$

Average stress in specimen:

$$(2.8) \quad \sigma(t) = \frac{[\sigma_1(t) + \sigma_2(t)]}{2} = \frac{A_0 E_0}{2A} [\varepsilon_i(t) + \varepsilon_r(t) + \varepsilon_t(t)]$$

When the stress pulse wave propagates several times to and fro in the specimen, the stress equilibrium state is established. In this case, three strain are equal as shown in Equ.8.

$$(2.9) \quad \varepsilon_i + \varepsilon_r = \varepsilon_t$$

Thus, by submitting equ.8 to equ.1~7, the following equations can be achieved.

$$(2.10) \quad \dot{\varepsilon}(t) = -\frac{2C_0}{L} \varepsilon_r(t)$$

$$(2.11) \quad \varepsilon(t) = -\frac{2C_0}{L} \int_0^t \varepsilon_r(t) dt$$

$$(2.12) \quad \sigma(t) = \frac{A_0 E_0}{A} \varepsilon_r(t)$$

Equ.10~12 can be used to calculate the stress, strain and strain rate in the research.

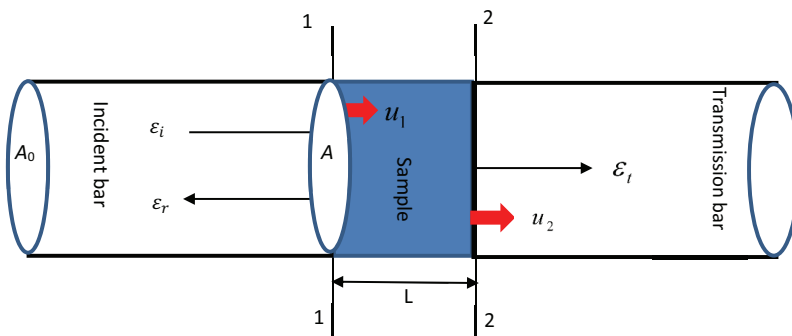


Figure 3. Schematic diagram of a sample under dynamic impact by SHPB

3. THE SPECIMEN PREPARATION

The specimens are made of cement, sand, pebble, and water. Table 1 shows the ratio of the materials. The specimens are made according to the international standard origination 3839-1977 file. Figure 3a illustrates the rare materials which are comprised of cement, sand, and pebble according to the ratio from SO 3839 file. Then the rare materials for making concrete are mixed together after pouring water (Figure 4b). The material will be stir for a while until it becomes evenly as illustrated in Figure 3b. After 24 hours, the mould for making concrete will be released as shown in Figure 3c. Then the concrete cubics will be kept for 28 days after it can be used as well concrete as shown in Figure 4d.

Table 1. The ratios of different materials for the concrete

Materials	Cement	Sand	Pebble	Water
Ration	1.540	3.770	6.350	1



(a) Rare material



(b) Mixing the material with water



(c) Concrete Cubic



(d) Concrete Cubic after 28 dyas

Figure 4 Concrete making process

The vertical coring machine (as shown in Figure 4a) was used to get a cylindrical specimen with a diameter of around 75mm. After that, the cutting machine was used to cut the cylindrical specimen to around 150mm in length (Figure5b). Thus, the coarse specimens were produced. In addition, the

grinding machine was used to make the specimen smoother (Figure 5c). The final rock samples for the uniaxial compressive strength test and the dynamic test are illustrated in Figure 6, while the details of the specimen parameters are listed in Table 2 for the uniaxial compressive strength test and Table 3 SHPB dynamic test.



(a) Coring machine (b) Cutting machine (c) grinding machine

Figure 5. Coring, cutting and grinding machine

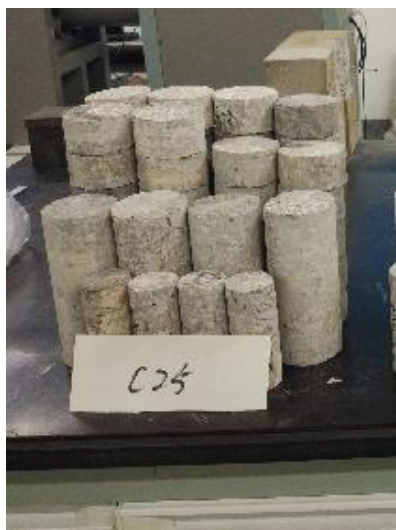


Figure 6. Rock sample for compressive strength

Table 2. Parameters of the specimens for compressive strength test under static loads

No	D/cm	L/cm	L/D	M/g	V/cm ³	ρ /g.cm ⁻³	Pv/m.s ⁻¹
1	7.430	15.340	2.065	1586	665.11	2.385	3150
2	7.420	14.960	2.016	1544	646.89	2.387	2895
3	7.440	15.236	2.048	1570	662.38	2.370	2458

Table 3. Parameters of the specimens for compressive strength test under dynamic loads

No	D/cm	L/cm	L/D	M/g	V/cm ³	ρ /g.cm ⁻³	Pv/m.s ⁻¹
1	7.420	3.600	0.485	371	155.67	2.383	2800
2	7.460	3.658	0.490	379	159.89	2.370	2450
3	7.340	3.550	0.484	353	150.21	2.350	2650

4. UNIAXIAL COMPRESSIVE STRENGTH TEST UNDER STATIC LOADS

Figure 7 shows the AW-2000D Rock mechanics testing machine for the uniaxial compressive test under static loads. The concrete specimen with a bottom diameter of 75mm and specimen height of 150mm is placed in the testing machine. Strain gages pasted on the specimen are used to collate the strain data during the test. The concrete specimen was placed between two plates. The top plate moves 0.02mm/s. Thus the force from the top plate is applied to the concrete.



Figure 7. Rock sample placed in TAW-2000D Rock mechanics testing machine

Figure 8 illustrates the experimental results, i.e. the fracture patterns of concrete. It can be seen that there are two main fracture from the top to the bottom of the specimen for Figure 8a. And there is

only one main fracture is produced vertically from the top to bottom of the specimen for Figure 8b. Figure 9 shown the Stress-strain curve for the uniaxial compressive strength test. According to the test, the calculated compressive strength σ_c , Young's modulus E and Poisson's ratio are listed in Table 4.



(a) Pattern A

(b) Pattern B

Figure 8. Rock failure patterns for the uniaxial compressive strength test

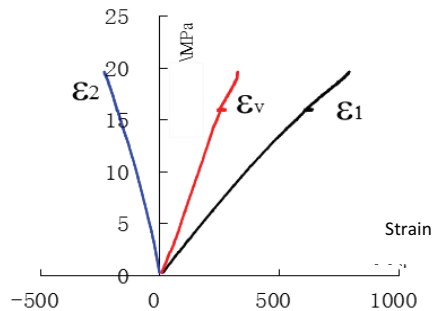


Figure 9. The Stress-strain curve for the uniaxial compressive strength test

Table 4. Experimental result for the uniaxial compressive strength test

Number	σ_c MPa	E GPa	ρ
C25-75-1	24.30	33.79	0.215
C25-75-2	22.69	32.42	0.234
C25-75-3	22.50	28.82	0.207

5. UNIAXIAL COMPRESSIVE STRENGTH TEST UNDER DYNAMIC LOADS

Figure 10 illustrates the Split Hopkinson Pressure Bar (SHPB) used for the compressive strength test. The parameters for the specimens used for the test are listed in table 3.



Figure 10. Split Hopkinson pressure bar (SHPB)

Figure 11 shows the experimental results for concrete under dynamic loads. The loading rates for the test are 27/s, 30.7/s, 37.3/s, and 51.4/s respectively. It indicates that with the loading rate increase, more fractures are produced. As shown in Figure 11(a), for the concrete under loading rate of 27/s, the fracture is produced along a diameter of the disc. The specimen is separated into two halves by the fracture. As for the concrete under the loading rate of 30.7/s, two main fractures are produced almost parallelly. The specimen is separated by the fracture into three parts. For the loading of 27, almost no fragment is produced. For the loading rate of 30.7, few of fragments can be seen.

While the loading rate increases to 37.3/s, the specimen are separated into many fragments as shown in figure 11c. As the loading rate continues to increase to 51.4/s, the specimen is scattered into fragments as shown in Figure 11d. Figure 11 illustrates the influence of the loading rates for the concrete in terms of compressive strength. It is obvious that stress is increasing with the increase of the strain. In addition, with the increase of the strain rate from 27/s to 51.4/s, the compressive strength become stronger and stronger. For both the stress-strain curves under different strain rates, the curves

show a typical brittle material failure process. Here, the stress-strain curves under the loading rate of 27/s is taken as an example.

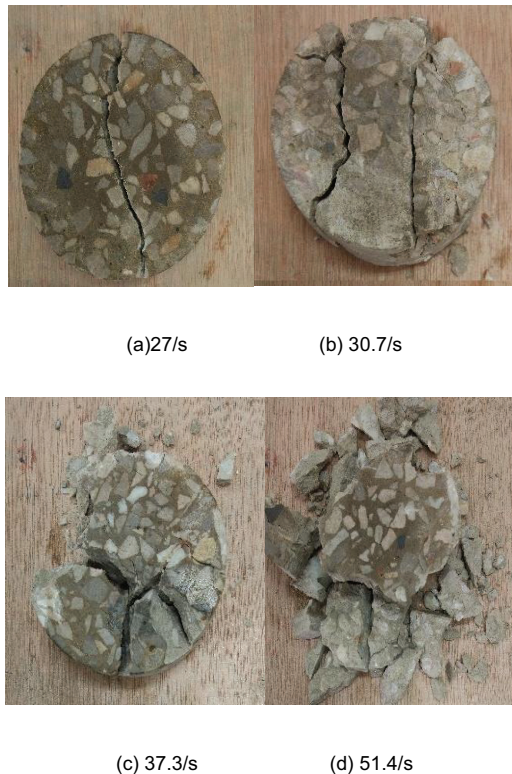


Figure 11. Fracture pattern for concrete under different dynamic loading rates

As can be seen in Figure 12, the behaviour of the concrete on dynamic load includes the following stages:

OA: As the strain increase, the existing micro-fractures are closed. The duration of this stage is very short.

AB: The stage of AB is considered as linear elastic and deformation is fully recoverable.

BD: the stage of BD is the nonlinear elastic stage. During this stage, the fracture propagates stably. If the load is removed, the fracture propagation will be stopped.

DF: DF is the unstable fracture propagation stage. D is the yielding point, and beyond this point, the permanent deformation develops and it is not recoverable even if the load is removed. At point F, the

allowable stress reaches the maximum limit, i.e. the material strength. Here is the uniaxial compressive strength. The failure of the concrete is expected to occur right after point F.

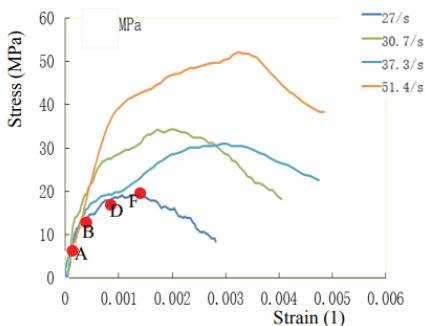


Figure 12. Stress-strain curves for concrete under different dynamic loading rates

As shown in Figure 12, all the curves include the four stages as described for the curve with a loading rate of 27/s. However, with the loading rate increase, the stress increases fast and the concrete fails at higher stress. Thus, the compressive strength is significantly influenced by the loading rate.

Table 5 listed the compressive strengths, the speed of the incident bar and stress rates for the test. It can be seen that the speed of the incident bar causes different stress rates. Then the stress rates influence the compressive strength and Young's modulus.

Figure 13, illustrates the influence of the loading rate on the compressive strength of concrete. Generally speaking, the compressive strength of the concrete increases rapidly with the increase of the strain rate. When the strain rate at 20/s, the compressive strength of concrete is almost the same as it under static loading. As the strain rate between 25 and 30, the strength increases faster compared with that after the strain rate of 35/s.

Table 5. Experimental results for the compressive strength test of concrete under dynamic loads

Number	σ_c	E	The speed of the incident bar (m/s)	$\dot{\epsilon}$
1	22.10	21.06	2.98	27.0
2	31.54	42.32	4.85	30.7
3	35.31	37.62	6.11	37.3
4	47.94	58.25	7.63	51.4

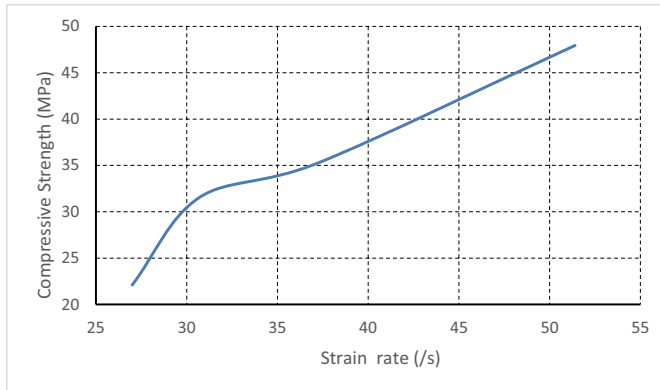


Figure 13. Influence of the loading rate on the compressive strength of concrete

6. CONCLUSION

As concrete is widely used in many geo-structures and the fracture of the concrete plays an important role in terms of the stability of the structure, this paper studies the fracture and fragmentation of concrete under static and dynamic loads and the influence of the loading rates on the compressive strength. The theories of calculation the static and dynamic parameters of concrete are introduced. The process of making concrete is described. After the concrete is made. The uniaxial compressive test of the concrete is conducted first. The compressive strength has been calculated and the fracture patterns of the concrete have been obtained. Then the Split Hopkinson Pressure Bar (SHPB) is employed to conduct the dynamic test of concrete. The concrete fractures under dynamic loads have been obtained. The influence of the strain rate on the dynamic concrete compressive strength has been studied. It is concluded that:

- The compressive strength of the concrete is significantly influenced by the strain rate. The compressive strength increases with the increase of the strain rate.
- The stress-strain curve of concrete under dynamic loads indicates a typical brittle material fracture process. It includes existing micro-fracture closure stage, linear-elastic stage, nonlinear-elastic stage, and post-failure stages.
- With the increase in loading rate, more fractures and fragments are produced.

Acknowledgements

This research presented in this study is partly supported by the following foundation and organizations: Research, National science foundation of China (Grant number: 11862010), Scientific research fund project of Yunnan provincial department of education (Grant No. 2020J0051). Start-up Fund for Talent of Kunming University of Science and Technology, Grant No. KKSJY201867017). Program for Innovative Research Team (in Science and Technology) in the University of Yunnan Province, and Yunnan Key Laboratory of Sino-German Blue Mining and Utilization of Special Underground Space, which are of greatly appreciated. Moreover, the authors would like to thank the anonymous reviewers for their valuable comments and constructive suggestion.

REFERENCES

1. Liu, H., Y. Kang, and P. Lin, Hybrid finite-discrete element modeling of geomaterials fracture and fragment muck-piling. *International Journal of Geotechnical Engineering*, 2013.
2. Zhao, J., Applicability of Mohr-Coulomb and Hoek-Brown strength criteria to the dynamic strength of brittle rock. *International Journal of Rock Mechanics and Mining Sciences*, 2000. 37(7): p. 1115-1121.
3. Zhang, Z., et al., Effects of loading rate on rock fracture: fracture characteristics and energy partitioning. *International Journal of Rock Mechanics and Mining Sciences*, 2000. 37(5): p. 745-762.
4. Dai, F., et al., Some fundamental issues in dynamic compression and tension tests of rocks using split Hopkinson pressure bar. *Rock mechanics and rock engineering*, 2010. 43(6): p. 657-666.
5. Dai, F., et al., Determination of dynamic rock mode-I fracture parameters using cracked chevron notched semi-circular bend specimen. *Engineering fracture mechanics*, 2011. 78(15): p. 2633-2644.
6. Eissa, E. and A. Kazi. Relation between static and dynamic Young's moduli of rocks. in *International Journal of Rock Mechanics and Mining Sciences & Geomechanics Abstracts*. 1988. Elsevier.
7. Mahanta, B., et al., Effects of strain rate on fracture toughness and energy release rate of gas shales. *Engineering Geology*, 2017. 218: p. 39-49.
8. Sukontasukkul, P., P. Nimityongskul, and S. Mindess, Effect of loading rate on damage of concrete. *Cement and Concrete Research*, 2004. 34(11): p. 2127-2134.
9. Zhang, Z., Laboratory studies of dynamic rock fracture and in-situ measurements of cutter forces for a boring machine. 2001.
10. Yin, Z., Dynamic compressive tests Gas-Containing Coal Using a Modified Split Hopkinson Pressure Bar System. 2019.

LIST OF FIGURES AND TABLES:

Figure 1. Geometrical model for the uniaxial compressive strength test

Figure 2. Schematic of conventional split Hopkinson pressure bar (SHPB)

Figure 3. Schematic diagram of a sample under dynamic impact by SHPB

Figure 4. Concrete making process

Figure 5. Coring, cutting and grinding machine

Figure 6. Rock sample for compressive strength

Figure 7. Rock sample placed in TAW-2000D Rock mechanics testing machine

Figure 8. Rock failure patterns for the uniaxial compressive strength test

Figure 9. The Stress-strain curve for the uniaxial compressive strength test

Figure 10. Split Hopkinson pressure bar (SHPB)

Figure 11. Fracture pattern for concrete under different dynamic loading rates

Figure 12. Stress-strain curves for concrete under different dynamic loading rates

Figure 13. Influence of the loading rate on the compressive strength of concrete

Table 1. The ratios of different materials for the concrete

Table 2. Parameters of the specimens for compressive strength test under static loads

Table 3. Parameters of the specimens for compressive strength test under dynamic loads

Table 4. Experimental result for the uniaxial compressive strength test

Table 5. Experimental results for the compressive strength test of concrete under dyn

Received: 04.03.2020 Revised: 04.07.2020

